Electrostatic Effects on the Stability of Condensed DNA in the Presence of Divalent Cations

John G. Duguid* and Victor A. Bloomfield
Department of Biochemistry, University of Minnesota, St. Paul, Minnesota 55108 USA

ABSTRACT Cylindrical cell model Poisson-Boltzmann (P-B) calculations are used to evaluate the electrostatic contributions to the relative stability of various DNA conformations (A, B, C, Z, and single-stranded (ss) with charge spacings of 3.38 and 4.2 Å) as a function of interhelix distance in a concentrated solution of divalent cations. The divalent ion concentration was set at 100 mM, to compare with our earlier reports of spectroscopic and calorimetric experiments, which demonstrate substantial disruption of B-DNA geometry. Monovalent cations neutralize the DNA phosphates in two ways, corresponding to different experimental situations: 1) There is no significant contribution to the ionic strength from the neutralizing cations, corresponding to DNA condensation from dilute solution and to osmotic stress experiments in which DNA segments are brought into close proximity to each other in the presence of a large excess of buffer. 2) The solution is uniformly concentrated in DNA, so that the neutralizing cations add significantly to those in the buffer at close DNA packing. In case 1), conformations with lower charge density (Z and ssDNA) have markedly lower electrostatic free energies than B-DNA as the DNA molecules approach closely, due largely to ionic entropy. If the divalent cations bind preferentially to single-stranded DNA or a distorted form of B-DNA, as is the case with transition metals, the base pairing and stacking free energies that stabilize the double helix against electrostatic denaturation may be overcome. Strong binding to the bases is favored by the high concentration of divalent cations at the DNA surface arising from the large negative surface potential; the surface concentration increases sharply as the interhelical distance decreases. In case 2), the concentration of neutralizing monovalent cations becomes very large and the electrostatic free energy difference between secondary structures becomes small as the interhelical spacing decreases. Such high ionic concentrations will be expected to modify the stability of DNA by changing water activity as well as by screening electrostatic interactions. This may be the root of the decreased thermal stability of DNA in the presence of high concentrations of magnesium ions.

INTRODUCTION

In recent work we have studied the structure and stability of DNA in the presence of divalent metal chlorides (Duguid et al., 1993, 1995). The solutions were rather concentrated (55 mg/ml DNA, 100 mM metal ion), as required by the Raman spectroscopy and differential scanning calorimetry techniques we used. Although divalent cations would normally be expected to stabilize the DNA double helix by screening electrostatic repulsions (Record et al., 1978), we found instead that high concentrations of transition metal cations destabilized the double helix, causing base unpairing and unstacking and backbone disorder at lower temperatures than observed with monovalent cations, or divalent alkaline earths. Several workers (Lyons and Kotin, 1965; Bauer, 1972; Ott et al., 1975; Blagoi et al., 1978) have observed that at low concentrations magnesium stabilizes the double helix, but at higher concentrations it lowers the helix coil melting temperature. This effect is even greater for transition metal ions that bind to the heterocyclic atoms of the DNA bases as well as to the phosphates (Blagoi et al., 1983; Eichhorn and Shin, 1968; Knoll et al., 1988).

In this paper we calculate the extent to which the electrostatic free energy of the polyelectrolyte solution may affect the relative stability of double-stranded and single-stranded DNA (ssDNA). We solve numerically the Poisson-Boltzmann equation with cylindrical cell model boundary conditions (Alfrey et al., 1951; Fuoss et al., 1951) for the double-stranded B, A, C, and Z conformations, and for ssDNA, to obtain the electrostatic internal energy, entropy, and free energy as functions of interhelix distance. The thermodynamic functions depend on the linear charge spacing and diameter of each form. For ssDNA these parameters are not tightly determined; we have used two sets that lead to quite different results.

We treat the monovalent cations that neutralize the DNA phosphates in two different ways, corresponding to different experimental situations. In the first, there is no significant contribution to the ionic strength from the neutralizing cations. This corresponds to DNA condensation from dilute solution and to osmotic stress experiments in which DNA segments are brought into close proximity to each other in the presence of a large excess of buffer. In the second case, the solution is uniformly concentrated in DNA, so that the neutralizing cations add significantly to those in the buffer: the bulk monovalent cation concentration increases as the distance between DNA rods decreases. This corresponds to our Raman spectroscopy and calorimetry experiments, and

Received for publication 12 October 1994 and in final form 22 February 1996.

Address reprint requests to Victor A. Bloomfield, Department of Biochemistry, University of Minnesota, 1479 Gortner Avenue, St. Paul, MN 55108. Tel.: 612-625-2268; Fax: 612-625-6775; E-mail: victor@biosci.cbs.umn.edu.

Dr. Duguid's present address is GeneMedicine, Houston, TX.

0006-3495/96/06/2838/09 $2.00

to experiments in which highly concentrated liquid crystalline phases are formed.

In solutions where the neutralizing cation from the DNA is negligible, the electrostatic free energy is lowest for the secondary structures with lowest charge density. We find that if the single-stranded form is relatively extended, with a linear charge spacing of 4.2 Å, the electrostatic free energy differences are such that, at small separations between DNA molecules, the combination of electrostatic and binding free energies may be sufficient to throw the equilibrium to the single-stranded form. However, if the single-stranded form is more compact, with a charge spacing of 3.38 Å (half that of B-DNA), the electrostatic free energy difference between single-stranded and B-forms tends to zero as separation decreases. In solutions where the concentration of neutralizing cation is taken into account, electrostatic contributions to the thermodynamic functions approach zero as DNA spacing becomes small. The very high concentration of monovalent cations near the DNA surface displaces the divalent cations from the surface under such circumstances.

NUMERICAL SOLUTION OF THE POISSON-BOLTZMANN EQUATION

The general form of the Poisson-Boltzmann equation for the potential ψ is

$$\nabla^2\psi = -\frac{4\pi}{\epsilon}\sum_i Z_i q c_{i,bulk}\exp\left(-\frac{Z_i q\psi}{k_B T}\right), \quad (1)$$

where ϵ is the dielectric constant, $Z_i q$ is the charge of ionic species i, $c_{i,bulk}$ is the concentration of each species (ions/ml), k_B is the Boltzmann constant, and T is the temperature of the solution. For cylindrical geometry the equation may be written in reduced units as

$$\frac{\partial^2\Phi}{\partial z^2} = -\frac{e^{2z}}{2I}\sum_i Z_i C_{i,bulk}\exp(-Z_i\Phi), \quad (2)$$

where Φ is the reduced potential, $\Phi = q\psi/k_B T$, and $z = \ln\kappa r$, where κ is the inverse Debye-Hückel screening length and r is the distance from the cylinder axis. The ionic strength of the solution is I, and the C_i's are molar concentrations.

Equation 2 must be solved subject to suitable boundary conditions. At the surface of a cylindrical rod, the boundary condition is

$$\left.\frac{\partial\Phi}{\partial z}\right|_{z=\ln\kappa a} = -2\xi, \quad (3)$$

where a is the radius of the cylinder, $\xi = q^2/\epsilon k_B T b$, and b is the average linear charge spacing between DNA phosphate charges. For an isolated rod, the change in potential with respect to distance approaches a limiting value:

$$\left.\frac{\partial\Phi}{\partial z}\right|_{z\to\infty} = -\frac{e^2 K_1}{K_0}, \quad (4)$$

where $K_0(z)$ and $K_1(z)$ are modified Bessel functions. For parallel rods whose centers are separated by a distance R, the potential between two rods is a minimum at $R/2$:

$$\left.\frac{\partial\Phi}{\partial z}\right|_{z=\ln\kappa R/2} = 0. \quad (5)$$

We solved these equations as previously described (Bloomfield et al., 1980) using Runge-Kutta numerical integration (Press et al., 1986). For the case of the isolated rod, this involves picking a very small value of Φ and an initial large value of z ($z_{initial}$). Equation 2 is then integrated from $z_{initial}$ to the surface of the cylinder, and $z_{initial}$ is modified iteratively until the integration satisfies the surface boundary condition Eq. 3 to within 0.1%. For equally spaced rods, an initial value of Φ ($\Phi_{initial}$) is chosen, and Eq. 2 is integrated from $R/2$ to the cylindrical surface. $\Phi_{initial}$ is adjusted iteratively until Eq. 3 is satisfied to within 0.1%. Our calculations were validated by comparison with those of Stigter (1975, 1982).

The reduced potential as a function of distance from the surface of the cylinder is then used to calculate the electrostatic free energy (G_{elec}) of the system. This is the work required to place a charged cylinder in a solution of counter-ions, co-ions, and an array of other charged rods if present. We employ a modification of a method previously used (Bloomfield et al., 1980; Oosawa, 1971), which begins with the familiar

$$G_{elec} = A_{elec} = U_{elec} - TS_{elec}. \quad (6)$$

The difference between the Gibbs energy G and the Helmholz energy A is assumed to be neglible. U_{elec} is the internal energy associated with introducing a charged rod into the system and is determined from the equation

$$\frac{U_{elec}}{k_B T} = \frac{1}{4\xi}\int_{\ln\kappa a}^{\ln\kappa r}\left(\frac{\partial\Phi}{\partial z}\right)^2 dz. \quad (7)$$

S_{elec} is the accompanying entropy change as the ionic species are redistributed around the charged cylinder. We used the equation recently derived by Stigter (1995), which refines previous expressions for the entropy. In our reduced units, it can be written

TABLE 1 DNA structural parameters used for Poisson-Boltzmann calculations

Secondary structure	Linear charge spacing b (Å)	Radius a (Å)	Surface area per DNA-P (Å^2)
A	1.28	11.5	92.5
B	1.69	9.5	101
C	1.66	9.5	99.1
Z	1.86	9.0	105
Single-stranded	4.20, 3.38	5.0, 7.0	132, 149

Dimensions of double-stranded DNA forms are from Lewin (1994), p. 120. Charge spacing of ssDNA is 4.2 Å from Record et al. (1978) or 3.38 Å, chosen to conserve charge in helix-coil transition of B-DNA. 7.0 Å radius of ssDNA is from Olmsted et al. (1991).

$$\frac{TS_{elec}}{k_BT} = \frac{1}{4I\xi}\sum_i C_{i0}\int_{\ln\kappa a}^{\ln\kappa r}[(z_i\phi + 1)e^{-z_i\phi+2z} - e^{2z}]dz, \quad (8)$$

where C_{i0} is the bulk concentration of ion species i, and I is the ionic strength. The upper bound ($\ln\kappa r$) of the integral in Eqs. 7 and 8 is $z_{initial}$ for the system containing an isolated rod, and $\ln(\kappa R/2)$ for an array of rods. The concentration of an ionic species i at any position z in the system is determined from

$$C_i = C_{i,bulk}e^{(-z_i\Phi)}. \quad (9)$$

Results from these calculations were identical, within roundoff error, to those we had previously obtained (Bloomfield et al., 1980) under the same ionic conditions when the previous expression for the entropy was used.

To compare the electrostatic free energies of double-stranded and ssDNA, and thus compute ΔG_{elec} upon strand separation accompanying thermal melting, we assumed that the single strands also formed a regular lattice of parallel cylindrical rods with no change in volume. Because there are twice as many rods (each with half the charge), the spacing is reduced by $\sqrt{2}$. All calculations were performed in 100 mM divalent metal chloride and 5 mM monovalent chloride at a temperature of 298°C and a dielectric constant of 78.44.

For those solutions in which cations from the DNA were taken into account, their concentration was computed as follows. Per phosphate, the volume of DNA is $\pi a^2 b$, and the volume of solution if the DNA cylinders are hexagonally arrayed with center-to-center distance R is $(\sqrt{3}/2)R^2b$. Thus the concentration of DNA phosphate, in moles per liter of solvent, is

$$C_{DNA-P} = \frac{1000}{N_A\left[\frac{\sqrt{3}}{2}R^2b - \pi a^2 b\right]}. \quad (10)$$

This is also the molar concentration of monovalent cations that neutralize the DNA.

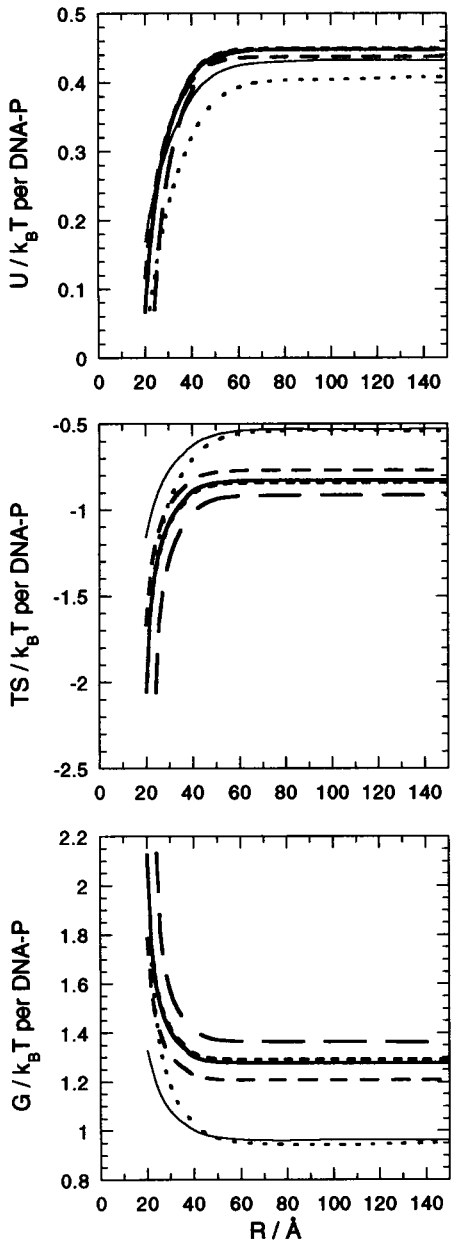

FIGURE 1 Dependence on center-to-center interhelical distance R of the electrostatic internal energy U, entropic energy TS, and free energy G, in units of k_BT per DNA phosphate, in solutions in which the monovalent cation contribution from the DNA is negligible. All solutions contain 100 mM divalent cation, 5 mM monovalent cation, and 205 mM monovalent anion. The line styles designate DNA secondary structures with parameters given in Table 1: *solid line*, B-DNA; *long dashes*, A-DNA; *medium dashes*, Z-DNA; *short dashes*, C-DNA (partly obscured by the B-DNA lines); *dots*, ssDNA with b = 3.38 Å and a = 7.0 Å; *thin solid line*, ssDNA with b = 4.2 Å and a = 5.0 Å.

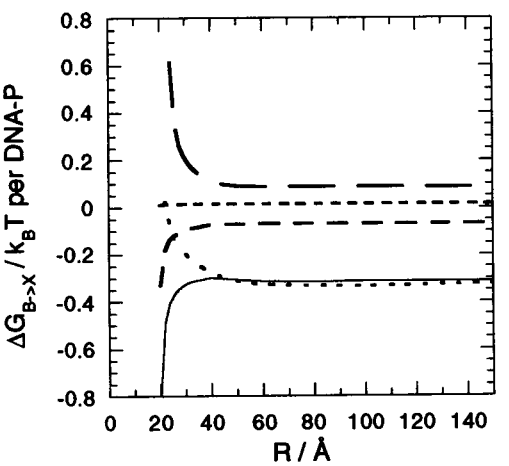

FIGURE 2 Electrostatic free energy change of B-DNA → X-DNA transition as a function of interhelical distance, in solutions in which the monovalent cation contribution from the DNA is negligible. The line styles designate the various final secondary structures X: *long dashes*, A-DNA; *medium dashes*, Z-DNA; *short dashes*, C-DNA; *dots*, ssDNA with b = 3.38 Å and a = 7.0 Å; *thin solid line*, ssDNA with b = 4.2 Å and a = 5.0 Å.

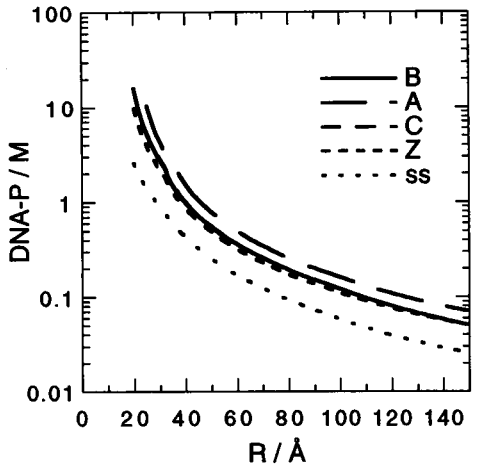

FIGURE 3 Moles of DNA phosphate per liter of solvent (equal to the concentration of monovalent cations contributed by the DNA) as a function of interhelical distance for the indicated DNA secondary structures.

RESULTS

We consider first the case in which the monovalent cations accompanying the DNA do not contribute significantly to the ionic strength. The radius a and charge spacing b of the DNA secondary structures are given in Table 1. Two sets of parameters have been used for ssDNA. The first, a = 5.0 Å and b = 4.2 Å, assumes a radius approximately half that of B-DNA and a charge spacing determined from early analysis of the salt dependence of the melting temperature of DNA (Record et al., 1978). The second, a = 7.0 Å and b = 3.38 Å, uses the radius proposed by Olmsted et al. (1991) and a charge spacing, twice that of B-DNA, close to the 3.5 Å used by these authors. This value of b is necessary for conservation of charge and DNA in the second case, considered below, in which the monovalent cations from the DNA must be considered in the solution composition.

Fig. 1 shows the electrostatic internal energy, entropy, and free energy of different DNA secondary structures as a function of interhelical distance. Perhaps contrary to naive expectation, U_{elec} decreases as the cylinders approach. The coulombic attraction between several DNA neighboring molecules and the counter-ions that they share more than compensates for the repulsive forces between the cylindrical polyanions. On the other hand, S_{elec} decreases as the cylinders are brought closer, because of the redistribution of counter-ions and co-ions in the presence of a charged polyelectrolyte. The concentration of counter-ions is very high near the polyanion surface and falls off at increasing distances; the opposite is true for co-ions. These concentration gradients, which become steeper as the cylinders are brought closer together, are entropically unfavorable. The entropy outweighs the internal energy, so G_{elec} increases as the DNAs approach.

Without taking into account the doubling of the concentration accompanying the helix-to-coil transition, we see that the relative electrostatic stability (ssDNA > Z-DNA > B-DNA ≈ C-DNA > A-DNA) is inversely related to the linear charge density at larger distances, and to the surface charge density as the charged cylinders approach each other (see Table 1). If the doubling of single-strand concentration

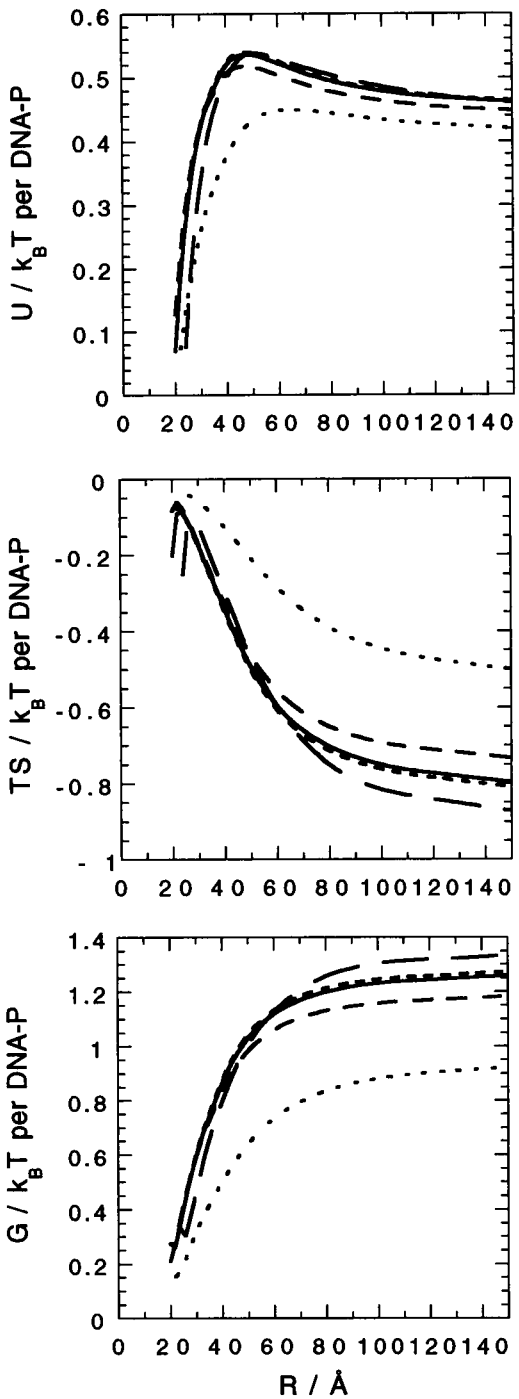

FIGURE 4 Dependence on center-to-center interhelical distance R of the electrostatic internal energy U, entropic energy TS, and free energy G, in units of k_BT per DNA phosphate, in solutions in which the monovalent cation contribution from the DNA is included. All solutions also contain 100 mM divalent cation, 5 mM monovalent cation, and 205 mM monovalent anion. *Solid line*, B-DNA; *long dashes*, A-DNA; *medium dashes*, Z-DNA; *short dashes*, C-DNA; *dots*, ssDNA with b = 3.38 Å and a = 7.0 Å.

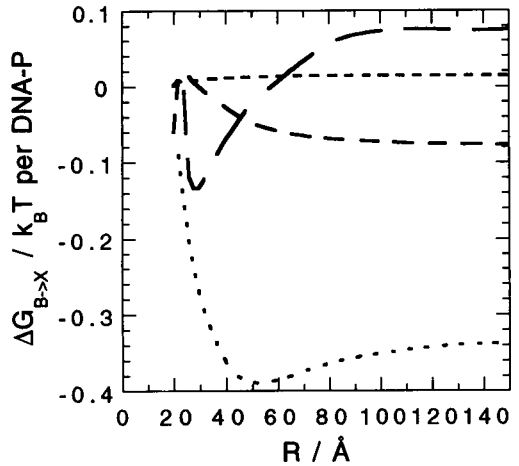

FIGURE 5 Electrostatic free energy change of B-DNA → X-DNA transition as a function of interhelical distance, in solutions in which the monovalent cation contribution from the DNA is included. The line styles designate the various final secondary structures X: *long dashes*, A-DNA; *medium dashes*, Z-DNA; *short dashes*, C-DNA; *dots*, ssDNA with b = 3.38 Å and a = 7.0 Å.

is recognized by applying a factor of $\sqrt{2}$ to the spacing, the free energy differential between ssDNA and dsDNA is reduced, but ssDNA is still more stable.

Subtracting G_{elec} for B-DNA from G_{elec} for the other conformations leads to Fig. 2, which shows ΔG_{elec} as a function of center-center distance for B-X transitions, where X is A, C, Z, or ssDNA. At interhelical spacings greater than 45 Å, the relative free energies of B-A, B-C, and B-Z transitions are independent of distance. Because of similar charge spacing and diameter in the B and C forms, ΔG_{elec} is independent of distance over the entire range. Z-DNA becomes strongly favored over the B form when the interhelical spacing is below 30 Å, whereas the A form becomes much less stable below 40 Å.

The relative electrostatic free energy between ss and dsDNA remains constant at duplex center-to-center distances greater than 60 Å, consistent with the experimental observation that DNA melting is independent of DNA concentration in dilute solutions. (Assuming hexagonal packing of cylindrical rods, 60 Å center-center separation corresponds to 115 mg/ml of B-DNA. The concentration increases as the inverse square of the separation.) For the ssDNA model with a = 5 Å and b = 4.2 Å, ΔG_{elec} increases slightly between 60 and 30 Å, then drops precipitously upon closer approach. This nonmonotonic behavior is the result of opposing, nonlinear dependence of ΔU_{elec} and ΔS_{elec}. For the ssDNA model with a = 7 Å and b = 3.38 Å, ΔG_{elec} becomes steadily less negative from 50 to 20 Å, becoming

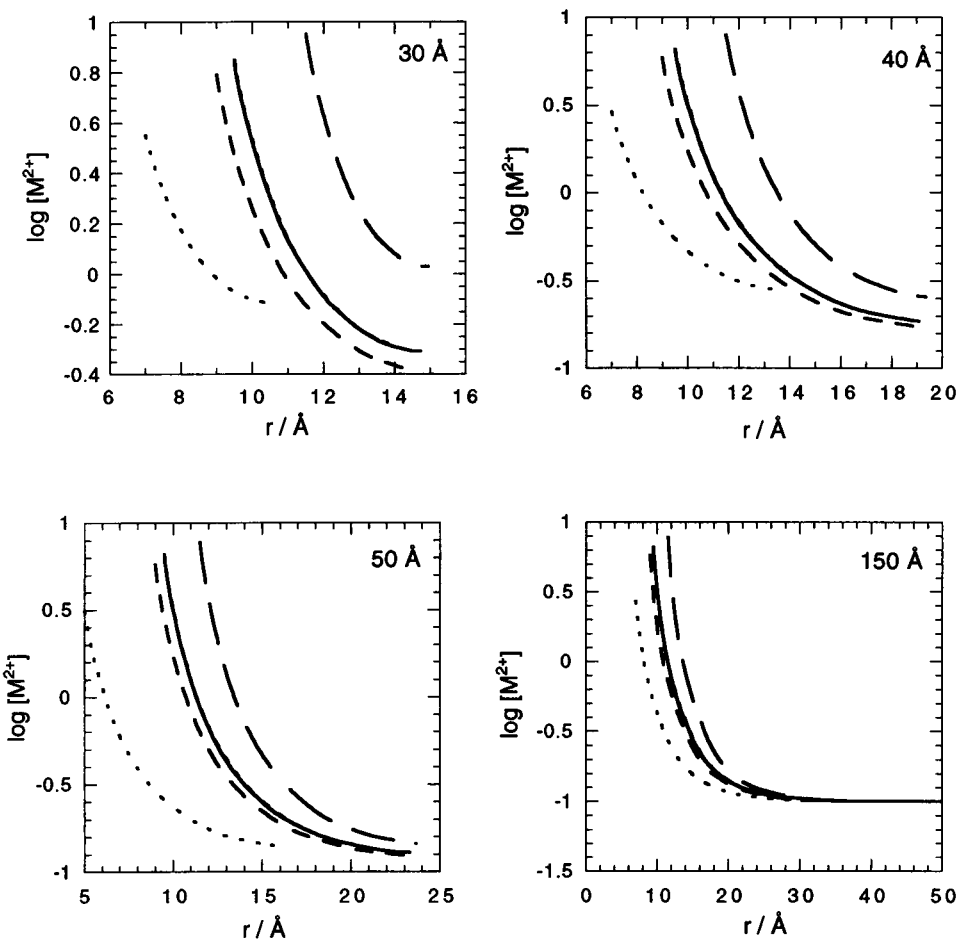

FIGURE 6 Logarithm of the molar concentrations of divalent cation as a function of distance from the center of the DNA helix, in solutions in which the monovalent cation contribution from the DNA is negligible. Interhelical distances are specified in the upper right-hand corner of each panel. Bulk ionic concentrations are 100 mM divalent cation, 5 mM monovalent cation, and 205 mM monovalent anion. *Solid line*, B-DNA; *long dashes*, A-DNA; *medium dashes*, Z-DNA; *short dashes*, C-DNA (sometimes obscured by the B-DNA lines); *dots*, ssDNA with b = 3.38 Å and a = 7.0 Å.

essentially zero at the latter value, because two single strands merge to become a rod with the same radius and charge density as B-DNA with this choice of parameters.

Although Figs. 1 and 2 suggest that duplex DNA should spontaneously undergo the helix-coil transition because of lower electrostatic free energy in the single-stranded form if ssDNA has an extended conformation with $b \approx 4.2$ Å, this does not normally happen. Base pairing and stacking contribute stabilizing free energy that more than compensates for electrostatics. However, if a cationic ligand can also disrupt base-base interactions, it can cause net destabilization. Depending on the nonelectrostatic free energy ΔG_{ne} of ligand-DNA interaction, the center-to-center distance at which duplex DNA becomes destabilized can extend anywhere from infinity to the diameter of the cylindrical rod. For example, if DNA has an enthalpy of melting of 6.7 kcal/mol bp and an entropy of melting of 19.3 cal/K mol bp (Duguid et al., 1995), single-strand DNA is less stable than B-DNA by ΔG of 475 cal, or 0.80 k_BT, per phosphate at 25°C. At a center-center spacing of 87 Å (~55 mg/ml DNA), ΔG_{elec} of ssDNA is about 0.35 k_BT lower, per phosphate, than ΔG_{elec} of B-DNA. Thus ΔG_{ne} favors B-DNA by 1.15 k_BT per phosphate. In combination with ΔG_{elec}, a very modest ligand binding constant ratio of exp(0.80) = 2.2, favoring ssDNA over B-DNA, would shift the equilibrium to the single-stranded side.

We next consider the second case, in which the monovalent cations accompanying the DNA contribute significantly to the ionic strength. In this case the only choice of ssDNA charge spacing that preserves electroneutrality and conservation of species in the helix-coil transition of B-DNA is $b = 3.38$ Å, twice that of B-DNA. For all secondary structures, the concentration of neutralizing cations, equal to that of DNA phosphates as calculated from Eq. 10, increases strongly as the interhelical distance decreases (Fig. 3). The electrostatic contributions to the thermodynamic functions are plotted in Fig. 4; the expected correlations with charge density are found at finite interhelical distances. As the rod-rod spacings approach zero, however, the electrostatic contributions disappear, because the very high neutralizing cation concentrations totally screen coulombic interactions. Fig. 5 shows the electrostatic component of ΔG for the transition from B-DNA to other forms. At 50 Å there is a significant ΔG_{elec} favoring ssDNA; this disappears as R decreases.The nonmonotonic behavior of these transitions arises because interactions depend mainly on linear charge density at long distances, but depend mainly on surface charge density at short distances, where screening due to the high monovalent cation concentration is also increasing rapidly.

The concentration of counter-ions near the surface of the DNA plays a major role in determining the distance dependence of the electrostatic free energy. We again consider first the case in which monovalent cations from the DNA are insignificant. Under our ionic conditions (100 mM divalent cation, 5 mM monovalent cation, and 205 mM monovalent anion), the Debye screening length κ^{-1} is 5.5 Å. As can be seen in Fig. 6, however, the concentration gradient close to the DNA surface is much steeper than the expo-

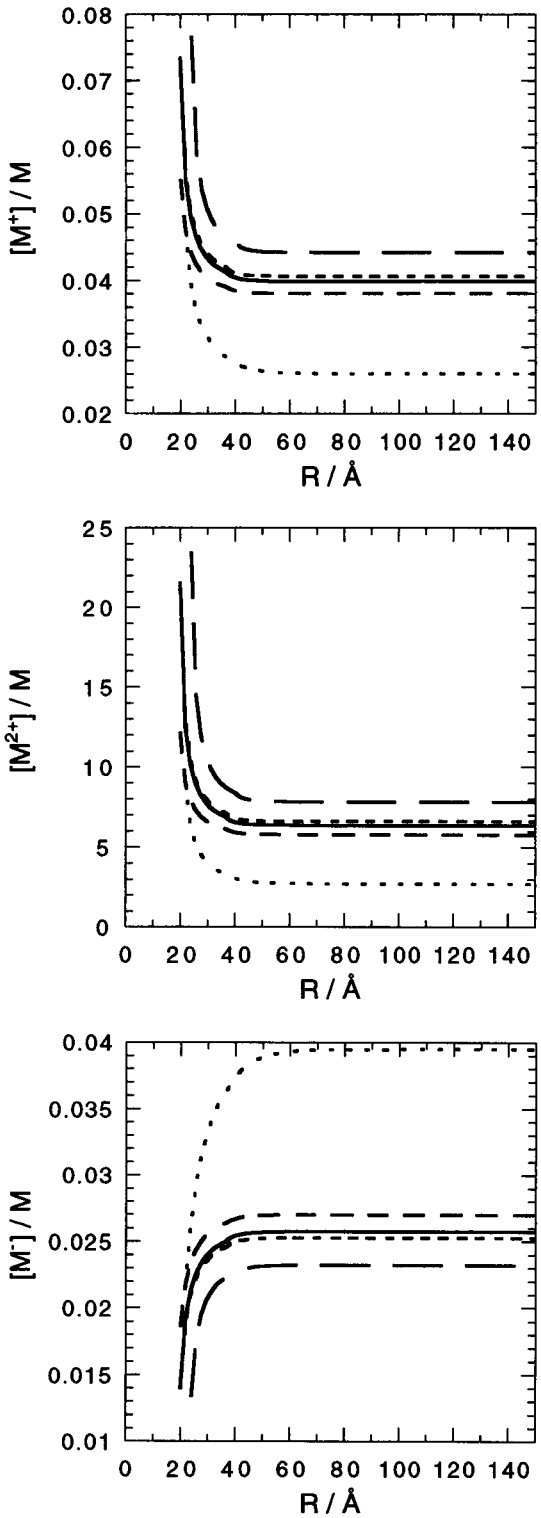

FIGURE 7 Surface concentrations of monovalent cation (M^+), divalent cation (M^{2+}), and monovalent anion (M^-) as functions of interhelical distance, in solutions in which the monovalent cation contribution from the DNA is negligible. Bulk ionic concentrations are 100 mM divalent cation, 5 mM monovalent cation, and 205 mM monovalent anion. *Solid line*, B-DNA; *long dashes*, A-DNA; *medium dashes*, Z-DNA; *short dashes*, C-DNA; *dots*, ssDNA with $b = 3.38$ Å and $a = 7.0$ Å.

nential Debye-Hückel screening. We calculate from Eq. 8 that the entropy associated with this steep ion gradient accounts for 70–99% of G_{elec}, depending on the interhelical spacing and DNA conformation.

In addition to providing a screening and entropic contribution to the electrostatic free energy, counter-ions may provide an additional effect by direct interaction at the surface of the DNA. In Fig. 7, we plot the concentration of counter-ions and co-ions at the surface (i.e., at $r = a$, using Eq. 9) as a function of interhelical spacing. The concentration of counter-ions at the surface is much greater than in the bulk solution. Under our standard conditions, the concentrations of divalent and monovalent cations reach over 20 and 0.07 M, respectively, at very short center-center spacings. Even in dilute solutions, the divalent cation concentration at the surface of dsDNA is greater than 5 M, consistent with numerous earlier calculations (Manning, 1978; Mills et al., 1985; Soumpasis, 1988) that showed high concentrations of counter-ions territorially bound near the DNA surface. Such high concentrations enhance the likelihood of direct interaction between bases and divalent cations, which, as pointed out above, may destabilize dsDNA.

In the second case, where monovalent cations from the DNA are included, the divalent ion concentration-distance profiles are qualitatively similar to the first case (compare Figs. 6 and 8), except that they are reduced severalfold, especially at small R, by competition from monovalent cations. The surface concentrations (Fig. 9) are dramatically different because of this competition. At small R, the very high monovalent cation concentration (Fig. 9, *top*) strongly displaces divalents (Fig. 9, *middle*), and the screening of repulsive coulombic interactions permits the closer approach of anions (Fig. 9, *bottom*).

DISCUSSION

We have shown that the electrostatic stability of single-stranded DNA, relative to double-stranded conformations, changes significantly with distance in concentrated solutions of divalent cations, particularly if the ssDNA is extended so that its linear charge density is low. At the small distances characteristic of condensed or tightly packaged DNA, ssDNA becomes markedly more stable electrostatically than B-DNA if close packing is local and the overall solution is dilute in DNA, so that neutralizing monovalent cations from the DNA do not significantly alter the ionic strength. Although strand separation is resisted by base pairing and stacking, these stabilizing interactions may be overcome if the divalent cations bind preferentially to ssDNA or to a distorted form of B-DNA. There is ample

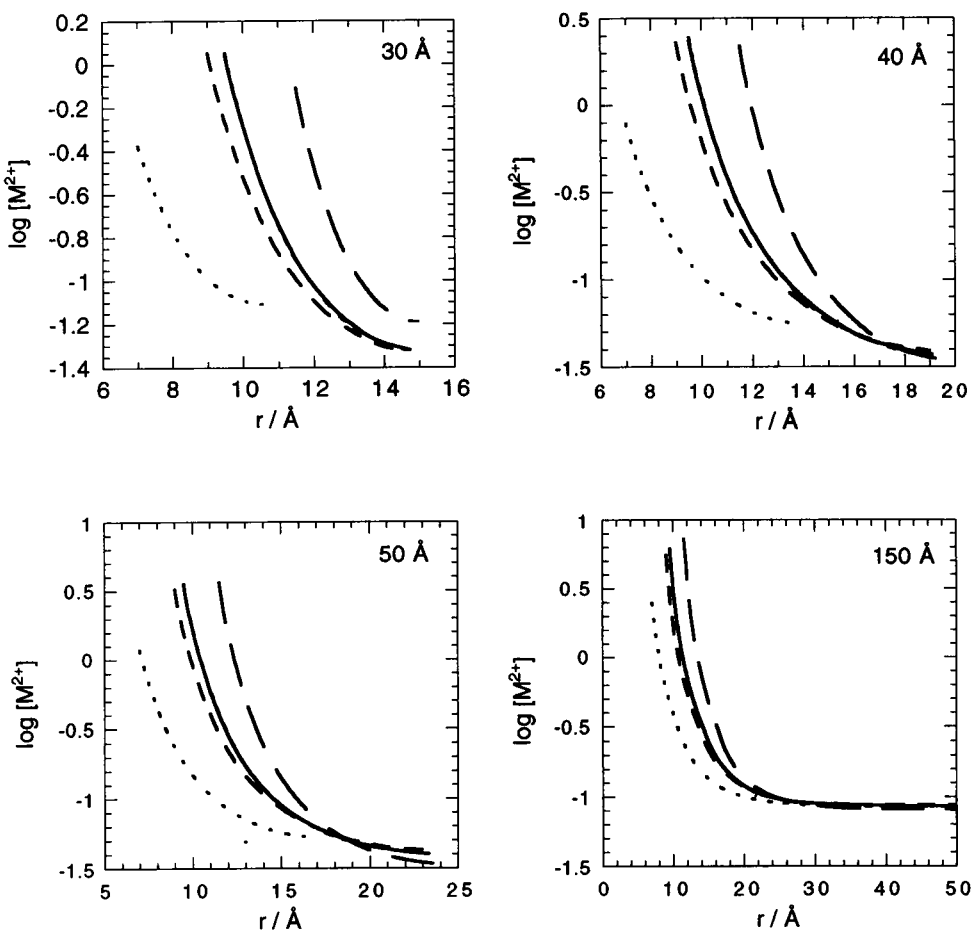

FIGURE 8 Logarithm of the molar concentrations of divalent cation as a function of distance from the center of the DNA helix, in solutions in which the monovalent cation contribution from the DNA is included. Interhelical distances are specified in the upper right-hand corner of each panel. All solutions also contain 100 mM divalent cation, 5 mM monovalent cation, and 205 mM monovalent anion. *Solid line*, B-DNA; *long dashes*, A-DNA; *medium dashes*, Z-DNA; *short dashes*, C-DNA (sometimes obscured by the B-DNA lines); *dots*, ssDNA with b = 3.38 Å and a = 7.0 Å.

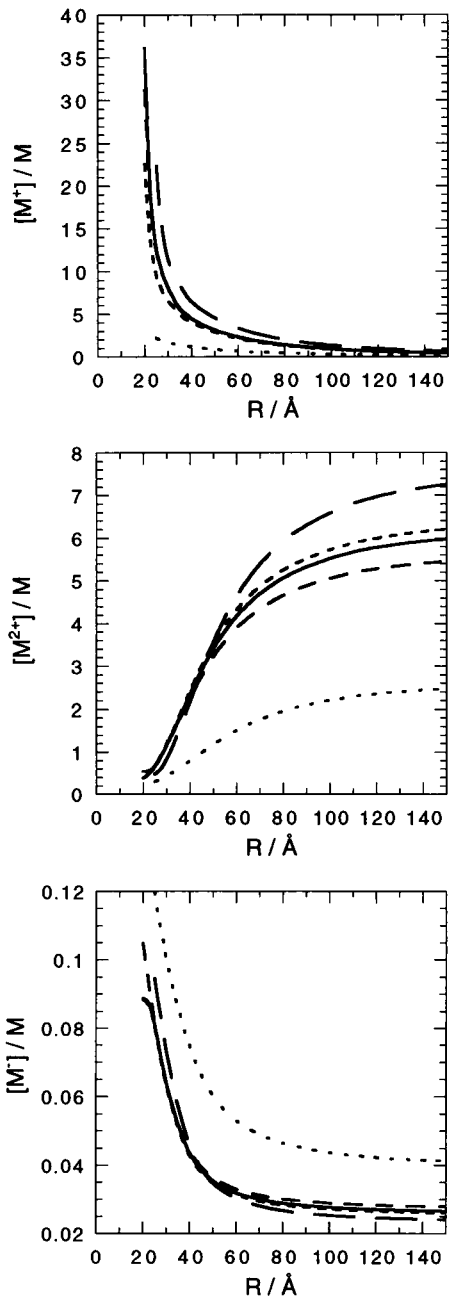

FIGURE 9 Surface concentrations of monovalent cation (M^+), divalent cation (M^{2+}), and monovalent anion (M^-) as functions of interhelical distance, in solutions in which the monovalent cation contribution from the DNA is included. All solutions also contain 100 mM divalent cation, 5 mM monovalent cation, and 205 mM monovalent anion. *Solid line*, B-DNA; *long dashes*, A-DNA; *medium dashes*, Z-DNA; *short dashes*, C-DNA; *dots*, ssDNA with b = 3.38 Å and a = 7.0 Å.

evidence that this occurs with divalent transition metals (Eichhorn and Shin, 1968; Knoll et al., 1988; Duguid et al., 1993, 1995). It is also intriguing that there is a class of "metal-responsive genes" that can be induced by different divalent metals with the strength of induction following the order Hg > Cd > Pb > Cu > Ni > Zn > Mg (Yiangou et al., 1991). Because this order is similar to that of effectiveness of DNA helix perturbation, it may be that our proposed mechanism has some direct biological relevance.

Our calculations show that the stability of ssDNA is greater relative to B-DNA, the more extended the ssDNA. Although recent analysis (Olmsted et al., 1991) shows that 3.5 Å may be a better value than 4.2 Å for the linear charge spacing b, the flexibility of ssDNA suggests that b could increase with little cost in free energy if other countervailing sources of free energy were present.

We should note that any DNA conformation with lower linear charge density than B-DNA will become more stable as the concentration increases; formation of single strands is not required. Indeed, the rapid recovery of normal B-form spectra upon lowering the temperature or adding EDTA to apparently "melted" DNA (Eichhorn and Shin, 1968; Knoll et al., 1988) argues against extensive strand separation.

When the DNA concentration is uniformly high throughout the solution, the concentration of neutralizing monovalent cations becomes very large and the electrostatic free energy difference between secondary structures becomes small as the interhelical spacing decreases. At these very high ionic concentrations, the Poisson-Boltzmann theory becomes quantitatively unreliable. However, the very presence of such high ionic concentrations will be expected to modify the stability of DNA by changing water activity as well as by screening electrostatic interactions. This may be the root of the decreased thermal stability of DNA in the presence of high concentrations of Mg^{2+} (Lyons and Kotin, 1965; Bauer, 1972; Ott et al., 1975; Blagoi et al., 1978).

These calculations are idealized in many ways. We use the simplest nonlinear Poisson-Boltzmann cylindrical cell model treatment, modeling the DNA as a uniformly charged cylinder on a regular lattice. We have treated the ions as spheres of zero radius. We have not attempted to treat the geometrical arrangement of phosphate charges in greater detail, or to use a distance-dependent dielectric constant, both of which have been shown to lead to significant variation in calculations of the relative stability of B- and Z-DNA conformations (Frank-Kamenetskii et al., 1987; Fenley et al., 1990). The values of the charge spacing and radii for ssDNA are simply illustrative and may be quite different for dilute solutions of DNA in monovalent salt than for concentrated, divalent salt solutions.

It is well known that at very high ionic concentrations, the Poisson-Boltmann approach becomes inadequate because of its neglect of excluded volume and electrostatic correlations between the mobile ions (Anderson and Record, 1990). Comparisons of Poisson-Boltzmann and Monte Carlo calculations (Le Bret and Zimm, 1984; Mills et al., 1985; Lamm et al., 1994) show that the former underestimates cation concentrations near the DNA surface by 5–15%. The discrepancy decreases with increasing counter-ion size, because of compensation of excluded volume and ionic correlation effects (Mills et al., 1985). Without detailed calculations, we cannot state with confidence how a more realistic treatment would affect the predicted relative stabilities of different DNA secondary structures. If the Poisson-Boltzmann

theory underestimates the concentration of counter-ions near the DNA surface, it probably underestimates the internal energy and overestimates the entropic contributions to stability. Because the entropic contribution is the greater part of the whole (Figs. 1 and 4), the net effect is probably a moderate overestimate of the relative stability of ssDNA relative to double-stranded forms. However, this is only conjecture.

We have also not attempted in this paper to calculate the forces required to achieve a given distance between DNA helices in hexagonal array, as measured in osmotic stress experiments (Rau et al., 1984; Rau and Parsegian, 1992a,b). Although such calculations could be made within the Poisson-Boltzmann framework, it is clear that a proper explanation of both repulsive and attractive interhelical forces can be achieved only by consideration of correlated counterion fluctuations (e.g., Nilsson et al., 1991) or by the hydration force mechanism promulgated by Rau, Parsegian, and their collaborators.

Thus, our calculations should be regarded as providing proof of principle, rather than highly accurate free energies. However, we believe that they provide a plausible explanation for a variety of experimental observations.

We are grateful to Dr. Ioulia Rouzina for helpful discussions.

This research was supported by National Institutes of Health research grant GM28093 to VAB, and by a Molecular Biophysics Predoctoral Traineeship (National Institutes of Health GM08277) to JGD.

REFERENCES

Alfrey, T., Jr., P. W. Berg, and H. Morawetz. 1951. The counterion distribution in solutions of rod-shaped polyelectrolytes. *J. Polym. Sci.* 7:543–547.

Anderson, C. F., and M. T. Record, Jr. 1990. Ion distributions around DNA and other cylindrical polyions: theoretical descriptions and physical implications. *Annu. Rev. Biophys. Biophys. Chem.* 19:423–465.

Bauer, W. 1972. Premelting unwinding of the deoxyribonucleic acid duplex by aqueous magnesium perchlorate. *Biochemistry.* 11:2915–2920.

Blagoi, Y. P., V. A. Sorokin, V. A. Valeev, and G. O. Gladchenko. 1983. Effects of calcium and manganese ions on the helix-coil transition of DNA. *Biopolymers.* 22:1641–1656.

Blagoi, Y. P., V. A. Sorokin, V. A. Valeyev, S. A. Khomenko, and G. O. Gladchenko. 1978. Magnesium ion effect on the helix-coil transition of DNA. *Biopolymers.* 17:1103–1118.

Bloomfield, V. A., R. W. Wilson, and D. C. Rau. 1980. Polyelectrolyte effects in DNA condensation by polyamines. *Biophys. Chem.* 11:339–343.

Duguid, J., V. Bloomfield, J. Benevides, and G. Thomas, Jr. 1993. Raman spectroscopy of DNA-metal complexes. I. Interactions and conformational effects of the divalent cations: Mg, Ca, Sr, Ba, Mn, Co, Ni, Cu, Pd, and Cd. *Biophys. J.* 65:1916–1928.

Duguid, J., V. A. Bloomfield, J. M. Benevides, and G. J. Thomas, Jr. 1995. Raman spectroscopy of DNA-metal complexes. II. The thermal denaturation of DNA in the presence of Sr^{2+}, Ba^{2+}, Mg^{2+}, Ca^{2+}, Mn^{2+}, Co^{2+}, Ni^{2+}, and Cd^{2+}. *Biophys. J.* 69:2623–2641.

Eichhorn, G. L., and Y. A. Shin. 1968. Interaction of metal ions with polynucleotides and related compounds. XII. The relative effect of various metal ions on DNA helicity. *J. Am. Chem. Soc.* 90:7323–7328.

Fenley, M. O., G. S. Manning, and W. K. Olson. 1990. A numerical counterion condensation analysis of the B-Z transition of DNA. *Biopolymers.* 30:1205–1213.

Frank-Kamenetskii, M. D., V. V. Anshelevich, and A. V. Lukashin. 1987. Polyelectrolyte model of DNA. <Translation> *Soviet Physics—Uspekhi.* 151:595–618.

Fuoss, R. M., A. Katchalsky, and S. Lifson. 1951. The potential of an infinite rod-like molecule and the distribution of the counterions. *Proc. Natl. Acad. Sci. USA.* 37:579–589.

Knoll, D. A., M. G. Fried, and V. A. Bloomfield. 1988. Heat-induced DNA aggregation in the presence of divalent metal salts. *In* Structure and Expression: DNA and Its Drug Complexes. Adenine Press, Albany. 123–145.

Lamm, G., L. Wong, and G. Pack. 1994. Monte Carlo and Poisson-Boltzmann calculations of the fraction of counterions bound to DNA. *Biopolymers.* 34:227–237.

Le Bret, M., and B. H. Zimm. 1984. Monte Carlo determination of the distribution of ions about a cylindrical polyelectrolyte. *Biopolymers.* 23:271–286.

Lewin, B. M. 1994. Genes V. Oxford University Press, New York.

Lyons, J. W., and L. Kotin. 1965. The effect of magnesium ion on the secondary structure of deoxyribonucleic acid. *J. Am. Chem. Soc.* 87: 1781–1785.

Manning, G. S. 1978. The molecular theory of polyelectrolyte solutions with applications to the electrostatic properties of polynucleotides. *Q. Rev. Biophys.* 11:179–246.

Mills, P., C. F. Anderson, and M. T. Record, Jr. 1985. Monte Carlo studies of counterion-DNA interactions. Comparison of the radial distribution of counterions with predictions of other polyelectrolyte theories. *J. Phys. Chem.* 89:3984–3994.

Nilsson, L. G., L. Guldbrand, and L. Nordenskjöld. 1991. Evaluation of the electrostatic osmotic pressure in an infinite system of hexagonally oriented DNA molecules. A Monte Carlo simulation. *Mol. Phys.* 72:177–192.

Olmsted, M. C., C. F. Anderson, and M. T. Record, Jr. 1991. Importance of oligoelectrolyte end effects for the thermodynamics of conformational transitions of nucleic acid oligomers: a grand canonical Monte Carlo analysis. *Biopolymers.* 31:1593–1604.

Oosawa, F. 1971. Polyelectrolytes. Marcel Dekker, New York.

Ott, G. S., R. Ziegler, and W. R. Bauer. 1975. The DNA melting transition in aqueous magnesium salt solutions. *Biochemistry.* 14:3431–3438.

Press, W. H., B. P. Flannery, S. A. Teukolsky, and W. T. Vetterling. 1986. Numerical Recipes: The Art of Scientific Computing. Cambridge University Press, Cambridge.

Rau, D. C., B. K. Lee, and V. A. Parsegian. 1984. Measurement of the repulsive force between polyelectrolyte molecules in ionic solution: hydration forces between parallel DNA double helices. *Proc. Natl. Acad. Sci. USA.* 81:2621–2625.

Rau, D. C., and V. A. Parsegian. 1992a. Direct measurement of the intermolecular forces between counterion-condensed DNA double helices. Evidence for long range attractive hydration forces. *Biophys. J.* 61:246–259.

Rau, D. C., and V. A. Parsegian. 1992b. Direct measurement of temperature-dependent solvation forces between DNA double helices. *Biophys. J.* 61:260–271.

Record, M. T., Jr., C. F. Anderson, and T. M. Lohman. 1978. Thermodynamic analysis of ion effects on the binding and conformational equilibria of proteins and nucleic acids: the roles of ion association or release, screening, and ion effects on water activity. *Q. Rev. Biophys.* 11:103–178.

Soumpasis, D. M. 1988. Salt dependence of DNA structural stabilities in solution. Theoretical predictions versus experiments. *J. Biomol. Struct. Dyn.* 6:563–574.

Stigter, D. 1975. The charged colloidal cylinder with a Gouy double layer. *J. Colloid Interface Sci.* 53:296–306.

Stigter, D. 1982. Coil expansion in polyelectrolyte solutions. *Macromolecules.* 15:635–641.

Stigter, D. 1995. Evaluation of the counterion condensation theory of polyelectrolytes. *Biophys J.* 69:380–388.

Yiangou, M., X. Ge, K. C. Carter, and J. Papaconstantinou. 1991. Induction of several acute-phase protein genes by heavy metals: a new class of metal-responsive genes. *Biochemistry.* 30:3798–3806.